

DEVELOPMENT PATH OF LOW ASPECT RATIO TOKAMAK POWER PLANTS

by

R.D. STAMBAUGH, V.S. CHAN, R.L. MILLER, P.M. ANDERSON, H.K. CHIU,
S.C. CHIU, C.B. FOREST, C.M. GREENFIELD, T.H. JENSEN, R.J. La HAYE,
L.L. LAO, Y.R. LIN-LIU, A. NEREM, R. PRATER, P.A. POLITZER,
H. ST. JOHN, M.J. SCHAFFER, G.M. STAEBLER, T.S. TAYLOR,
A.D. TURNBULL, C.P.C. WONG

MARCH 1997

DISCLAIMER

This report was prepared as an account of work sponsored by an agency of the United States Government. Neither the United States Government nor any agency thereof, nor any of their employees, makes any warranty, express or implied, or assumes any legal liability or responsibility for the accuracy, completeness, or usefulness of any information, apparatus, produce, or process disclosed, or represents that its use would not infringe privately owned rights. Reference herein to any specific commercial product, process, or service by trade name, trademark, manufacturer, or otherwise, does not necessarily constitute or imply its endorsement, recommendation, or favoring by the United States Government or any agency thereof. The views and opinions of authors expressed herein do not necessarily state or reflect those of the United States Government or any agency thereof.

GA-A22565

DEVELOPMENT PATH OF LOW ASPECT RATIO TOKAMAK POWER PLANTS

by

**R.D. STAMBAUGH, V.S. CHAN, R.L. MILLER, P.M. ANDERSON, H.K. CHIU,
S.C. CHIU, C.B. FOREST, C.M. GREENFIELD, T.H. JENSEN, R.J. La HAYE,
L.L. LAO, Y.R. LIN-LIU, A. NEREM, R. PRATER, P.A. POLITZER,
H. ST. JOHN, M.J. SCHAFFER, G.M. STAEBLER, T.S. TAYLOR,
A.D. TURNBULL, C.P.C. WONG**

This is a preprint of a paper to be presented at the
Fourth International Symposium on Fusion Nuclear
Technology, April 6–11, 1997, Tokyo, Japan and to be
published in *Fusion Engineering and Design*.

Work supported by
the U.S. Department of Energy
under Contract No. DE-AC03-89ER51114

**GA PROJECTS 3466 and 4437
MARCH 1997**

ABSTRACT

Recent advances in tokamak physics indicate the spherical tokamak may offer a magnetic fusion development path that can be started with a small size pilot plant and progress smoothly to larger power plants. Full calculations of stability to kink and ballooning modes show the possibility of greater than 50% beta toroidal with the normalized beta [$\beta_N = \beta_T / (I/ab)$] as high as 10 and fully aligned 100% bootstrap current. Such beta values coupled with 2–3 T toroidal fields imply a pilot plant about the size of the present DIII-D tokamak could produce ~800 MW thermal, 160 MW net electric, and would have a ratio of gross electric power over recirculating power (Q_{PLANT}) of 1.9. The high beta values in the ST mean that E×B shear stabilization of turbulence should be 10 times more effective in the ST than in present tokamaks, implying that the required high quality of confinement needed to support such high beta values will be obtained. The anticipated beta values are so high that the allowable neutron flux at the blanket sets the device size, not the physics constraints. The ST has a favorable size scaling so that at 2–3 times the pilot plant size the Q_{PLANT} rises to 4–5, an economic range and 4 GW thermal power plants result. Current drive power requirements for 10% of the plasma current are consistent with the plant efficiencies quoted. The unshielded copper centerpost should have an adequate lifetime against nuclear transmutation induced resistance change and the low voltage, high current power supplies needed for the 12 turn TF coil appear reasonable. The favorable size scaling of the ST and the high beta mean that in large sizes, if the copper TF coil is replaced with a superconducting TF coil and a shield, the advanced fuel D-He³ could be burned in a device with $Q_{\text{PLANT}} \sim 4$. If the anticipated physics of the ST regime can be proven in near term experiments and engineering challenges (such as the high power density to be exhausted and centerpost neutronics issues) can be met, then the ST offers the possibility of a magnetic fusion development path with a minimal cost initial step and exciting further possibilities.

1. INTRODUCTION

The advantages of the spherical tokamak approach have been discussed for many years [1,2]. In recent years, interest in the ST approach has grown rapidly, spawning a number of workshops [3] and a number of new experimental machine proposals [4–6]. Reference [7] is a valuable review of the field. Some studies projecting the ST approach to burning plasma devices have appeared [8,9].

The ST approach minimizes the size of a tokamak power core by discarding components from the inner side of the plasma: no inboard blanket or shield, no inboard poloidal coil (PF) systems, no Ohmic heating (OH) solenoid, resulting in low aspect ratio tokamaks, with aspect ratio A generally less than 1.5. The only customary tokamak component that remains is a single-turn copper toroidal field (TF) coil centerpost.

The key to the ST approach is that the beta values made possible by the combination of high elongation and low aspect ratio are sufficiently high that limits on the neutron wall loading of the blankets determine the machine size [10,11].

2. STABILITY STUDIES

A relation for the β -limit as a function of aspect ratio is needed. Using poloidal circumference = $2\pi a [(1 + \kappa^2)/2]^{1/2}$, equilibrium theory and the definitions of the quantities involved give:

$$\beta_T \beta_p = 25 \left(\frac{1 + \kappa^2}{2} \right) \left(\frac{\beta_N}{100} \right)^2 . \quad (1)$$

Equation (1) squarely puts the major conflict in advanced tokamak design at any aspect ratio. One wants high β_T for fusion power and high β_p for high bootstrap fraction. But β_T and β_p trade-off against each other, given conventional β -limit scaling $\beta_N = \text{constant}$. The way to increase β_T and β_p *simultaneously* is to increase κ and β_N .

To determine $\beta_N(A)$, we have explored a range of equilibria at low A varying the pressure profile, the current profile, the plasma shape, and aspect ratio [12]. Equilibria with complete bootstrap alignment and bootstrap fraction f_{bs} 100% at aspect ratio of 1.4 have been obtained [13]. Kink modes with $n = 1, 2$, and 3 are stable (GATO [15]) for β_N of 8 or larger with wall stabilization for a moderately placed wall. Wall stabilization is also required for $n = 0$ axisymmetric modes. Two paths were pursued to optimize ballooning stability with fully driven bootstrap current. One used a finite pressure gradient at the plasma edge p'_{edge} as is usual in DIII-D H-mode. A stable equilibrium with $\beta_N = 10$ and finite p'_{edge}

(77% of the maximum p') has been found and confirmed by several different codes [12]. A second path optimized β_N with $p'_{edge} = 0$. Scanning δ at fixed $\kappa (=2.5)$, both β_N - and β_T - limits show a maximum at $\delta = 0.4$ owing to the competition between the stabilizing effect of a deeper magnetic well at higher δ and higher edge bootstrap current at lower δ . At fixed δ , both β_N - and

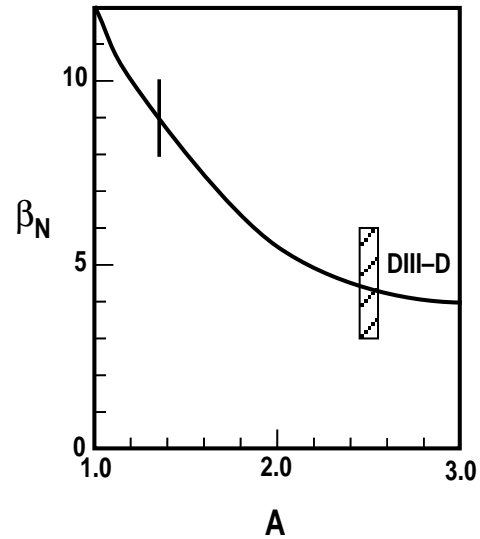


Fig. 1. The relation $\beta_N = 12/A$. Achieved values in DIII-D experiments are shown at $A = 2.5$. A range of theoretical calculations from Ref. [12] are shown at $A = 1.4$.

β_T - limits increase with κ . At $\kappa = 3$, equilibria with β_N exceeding 8 and β_T exceeding 50% with full bootstrap alignment are stable to $n = \text{infinity}$ ballooning modes. Our stability calculations [12] support a *specific advantage* of low aspect ratio in plasma stability. The function $\beta_N = 12/A$ passes through our theory results at $A = 1.4$ (Fig. 1) and the center of the range of data from DIII-D [15]; $\beta_N = 6$, more optimistic than our assumed function, has been achieved transiently and is expected to be stable in steady-state in second stable core VH-mode (SSC-VH [16], negative central shear mode [17]). Our axisymmetric stability calculations show $n = 0$ modes can be feedback stabilized up to $\kappa = 4$ for $\ell_i = 0.6$ and $r_{\text{wall}}/a = 1.5$. We chose $\kappa = 3$. Neoclassical tearing modes [18] can be expected to be stable since $q_{\text{min}} > 4$ everywhere [12] and the stabilizing Glasser term dominates at low A .

3. POWER GAIN

A large excess of fusion power P_F must be produced relative to the resistive power P_c in the TF centerpost. We calculated a “centerpost gain” (P_F/P_c) and looked at optimizations. The centerpost is a straight cylinder of radius R_c and height $h_c = 2 a\kappa$. No other inboard space allowance is taken. The centerpost current density is J_c and the fraction of the centerpost area that is copper is λ .

Using standard forms for the D–T fusion reactivity [19], the optimum D–T mix, $n_D = n_T = 1/2 n_e$, and parabolic profiles with exponents $S_n = 0.25$ and $S_T = 0.25$ to conform to the pressure profile in stability calculations, we express the fusion power P_F in terms of the volume average plasma toroidal β_T and the vacuum toroidal field B_T to keep contact with the β -limit scaling for higher aspect ratio tokamaks [20] $\beta_N \equiv \beta_T/(I_p/aB_T)$ (% ,MA,m,T). In our scoping studies, we used the relation $\beta_N = 12/A$ in Eq. (2) to allow a tradeoff of β_T and β_p with a basis point at our $\kappa = 3$, $\beta_N = 8.6$, $\beta_T = 56\%$, $f_{bs} = 100\%$ case. From a study of the dependence of f_{bs} on density and temperature scale lengths, we adopted profiles for which $L_n = L_T$ and for which the pressure profile was as broad as in the stability results. In this case $f_{bs} = 0.72 \beta_p/\sqrt{A}$. Using $\beta_N = 12/A$ in Eq. (1) to eliminate β_T in $P_F = 1.2 (\beta_T B_T^2)^2 V(\text{MW,T,m})$,

$$\frac{P_F}{P_c} = \frac{(1.2)(0.2)^4 \pi^5 \lambda}{\eta_c} \left(\frac{0.36[(1+\kappa^2)/2]}{\beta_p} \right)^2 \times J_c^2 R_c^4 \frac{(A-1)^2}{A^7} . \quad (2)$$

This relation implies an optimum aspect ratio of 1.4. The relation [Eq. (2)] shows a very strong economy of scale in the low aspect ratio approach since $P_F/P_c \propto R_c^4$.

A neutron wall loading constraint will be the limiting factor in performance. We take 8 MW/m² to be at the high end of possibility. The family of machines with constant wall loading is defined by $J_c^4 R_c^5 = \text{constant}$. With this constraint, the centerpost gain P_F/P_c will have the size scaling $R_c^{3/2}$, much weaker than the R_c^4 scaling considering only operation at the β -limit with a fixed J_c . We found that increasing κ from 2 to 3 is able to effect a factor 2 reduction in plasma and machine volume, providing strong motivation to increase the elongation.

4. INTEGRATED DESIGNS

We constructed a complete plant model in a spreadsheet. The current density J_c is adjusted to give the specified wall loading power. Some allowance for the elevated operating temperature of the centerpost is made by taking $\eta_c = 2.0 \times 10^{-2} \mu\Omega\text{m}$ and we took $\lambda = 0.8$. A water flow velocity $V_w = 10$ m/s always gives a small temperature rise. The twelve outer legs of the TF coil are sized to obtain a resistive dissipation equal to 0.5 of the centerpost power and the resulting cross-sections are modest (0.2 to 0.6 m on a side). The total voltage drop on the TF coil, V_{TF} , ranges from 9 to 6 V. With semiconductor power supplies for the TF with an internal voltage drop of about 1 V, we take the electrical efficiency of the TF power source to be $0.9 (1 - 1 \text{ V}/V_{TF})$.

We specify $f_{bs} = 0.9$ and compute $\beta_p = f_{bs} \sqrt{A}/0.72$. The β_T is calculated from Eq. (1) with $\beta_N = 12/A$. The safety factor q is always unrestrictive (~ 6). The product of central density n_0 and temperature T_0 is computed from β_T . We assume $T_0 = 25$ keV and calculate n_0 , which ranges from 4 to $2 \times 10^{20} \text{ m}^{-3}$. These densities range from 0.2 to 0.7 times the Greenwald limit $n_{GR} = I_p(\text{MA})/\pi a^2$.

We compute the power required P_{CD} to drive the remainder of the current $I_{CD} = I_p (1 - f_{bs})$ [21]. $P_{CD} = \bar{n} R_0 I_{CD}/\gamma$, where γ is the usual current drive figure of merit for the various current drive schemes evaluated at the volume average temperature and density [21]. The values P_{CD} were similar for the various rf and NBCD schemes; in our power balance, we used the NBCD result which ranged from 5 to 24 MW.

The electrical efficiency of the current drive system is taken as $\eta_{CD} = 0.4$. All other plant systems are assumed to require 7% of the gross electric power generated. So the power recirculating in the plant is $P_{RECIRC} = P_{CD}/\eta_{CD} + P_{TF}/\eta_{TF} + 0.07 P_{GROSS,E}$. A blanket multiplier $M = 1.25$ was taken. None of the power collected as heat ($P_\alpha + P_{CD,E} + P_{TF,E}$) was taken into the thermal cycle. The efficiency of the thermal cycle was taken as 46%. The gross electric power is $P_{GROSS,E} = [M(P_F - P_\alpha)]/0.46$. $Q_{PLANT} = P_{GROSS,E}/P_{RECIRC}$.

We found the low aspect ratio path does contain a small pilot plant type device and an attractive economy of scale to power plants (Fig. 2). All of the designs considered have in common $A = 1.4$, $\beta_T = 62\%$, $\beta_p = 1.48$, $f_{bs} = 0.90$, $\kappa = 3.0$, neutron power at blanket = 8 MW/m^2 . At $R_c \sim 0.2$ to 0.3 m, we find pilot plants with $P_F/P_c = 5$ to 10 and $Q_{PLANT} = 1$ to 2 .

At larger $R_c \sim 0.6$ to 0.8 m, we find a suitable range for a power plant with $P_F/P_c = 30$ to 45 and $Q_{PLANT} = 4$ to 5.

The wall loading constraint forces J_c to decrease as R_c increases. The pilot plants have $J_c = 80$ to 50 MA/m² and toroidal fields 2.9 to 2.7 T. The power plants have $B_0 = 2.2$ to 2.1 T and $J_c \sim 22$ to 16 MA/m². The centerpost power ranges from 60 MW in the pilot plant to 130 MW in the power plant. The plasma current ranges from 15 to 30 MA.

Taking account of bremsstrahlung and assuming $P_{RAD} = 25\%$ of the sum of $P_\alpha + P_{CD}$, we calculate the index of divertor power handling P/R_0 and find values ranging from 80 to 300 MW/m; P/R_0 in ITER is ~ 40 MW/m. It appears these devices will need to use a radiating mantle to deliver the power to the large area outer wall instead of trying to handle a majority of the power in the small divertor volume.

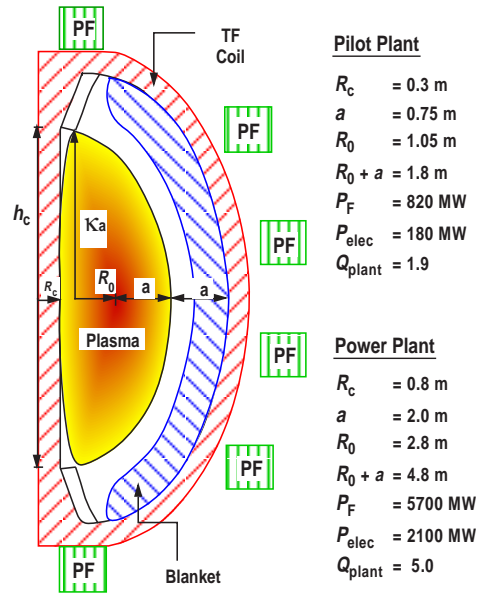


Fig. 2. An ST power plant is 2–3 times the linear dimension of an ST pilot plant. Both cases for $A = 1.4$, neutron wall load at the blanket 8 MW/m², $\beta_T = 62\%$, $\beta_p = 1.48$, $f_{bs} = 0.9$, $\kappa = 3.0$.

5. CONFINEMENT AND $E \times B$ SHEAR

We have examined operation at the β -limit. The total heating power $P_\alpha + P_{CD}$ has also been calculated so we can calculate the energy confinement time required to provide a steady-state at the β -limit. Those confinement times are then compared to the ITER89-P L-mode scaling [22] to define $H = \tau_E/\tau_{89P}$. The absolute energy confinement times are reasonable ranging from 0.4 to 0.9 s. An H factor of 5 in the pilot plant range and 3 in the power plant range is required.

Prospects for obtaining this required confinement quality are excellent. The transport barriers formed in H-mode, VH-mode, and negative central shear (NCS) mode all derive from stabilization of turbulence by sheared $E \times B$ flow [23]. Turbulence suppression is strong when the shearing rate $\omega_{E \times B}$ [24] exceeds the turbulence decorrelation rate (ω_T).

We have evaluated $\omega_{E \times B}$ in our highest β equilibrium and found values of 30 MHz in the high pressure gradient region near the outer midplane, 300 times the 100 kHz values in present experiments that achieve neoclassical transport levels. Our 1-D transport calculations (in a pilot plant size device with $B_T = 1.0$ T, $I_p = 5$ MA) find if ω_T is ≤ 60 kHz, a strong enough transport barrier forms. Assuming residual ion transport is neoclassical and electron transport is $10 \times$ ion transport, $\beta_T > 50\%$ results.

6. TECHNOLOGY ISSUES

We calculated the lifetime of the centerpost in the power plant ($R_c = 0.6$ m case) against the nuclear transmutation induced increase in resistance, using 2-D distributions of dpa calculated in an $R_c = 0.14$ m centerpost [25] adapted to our larger centerpost. One MW-yr/m² produces 10 dpa in the copper surface at the midplane. The change in resistivity per dpa is 2.8×10^{-10} Ω -m/dpa. With an 8 MW/m² neutron flux on the centerpost, we find a 10% increase in resistance in one year, 50% increase in 7 years, and a 100% increase in 22 years. The centerpost changeout time for economic reasons (too high P_c) would be ~ 7 years.

We also looked at the unusual low voltage, high current semiconductor power supplies needed for the one turn in each return leg TF coil. To keep reasonable the transmission line power losses, the power supplies must closely ring the device (5 m transmission line lengths) with a floor space requirement of 0.3 m²/MVA and a 6 m height.

7. PROSPECTS FOR ADVANCED FUEL BURNING

Because of the strong scaling of gain P_F/P_C with size ($\propto R_C^4$), the question naturally arises as to whether there is enough excess capacity in the ST at large size to burn advanced fuels like D–He³ despite their lower reactivity. A D–He³ system can produce as low as 1% of the neutron power from a D–T system, effectively removing centerpost radiation damage as a design issue. We developed the formula for fusion power from D–He³ [27] in terms of β and obtained $P_F = 0.016 (\beta_T B_T^2)^2$ (MW,T,m³) and proceeded to plant designs. We also looked at D–T systems in the large sizes required to shield a superconducting centerpost (Table I). The endpoint of a copper TF ST development path starting at small $R_C = 0.3$ m pilot plants could be superconducting STs with $R_C > 1.5$ m.

Table I
Devices at an 8 MW/m² Neutron Wall Load

Parameter	D–He ³		D–T
	Copper	Superconducting	Superconducting
R_C (m)	3	1.5	1.5
R_0 (m)	10.5	5.25	5.25
a (m)	7.5	3.75	3.75
J_C (MA/m ²)	6	$\geq 60^*$	$\geq 60^*$
Fusion power (MW)	23,000	1,400	13,700
Q_{PLANT}	3.4	4.3	12
Net electric power (MW)	7,600	500	5,800
Current drive power (MW)	105	42	43
I_p (MA)	175	73	44
B_0 (T)	3.2	2.7	1.6
τ_E (s)	5.7	8.1	1.5
H	2.1	4.5	2.0
P_F/A_{wall} (MW/m ²)	5.7	1.4	5.4 [†]
T_0 (keV)	100	60	25
n_0 (10 ²⁰ m ⁻³)	1.4	1.7	1.2

*Assuming one meter thick neutron shield.

[†]Neutron power at the blanket.

8. CONCLUSIONS

The key to the ST approach is that the beta values made possible by the combination of high elongation and low aspect ratio are sufficiently high that limits on the neutron wall loading of the blankets determine the machine size. The fusion power produced far exceeds the Ohmic losses in the copper TF coil. With no OH transformer, the ST devices are of necessity steady-state with full non-inductive current drive. High beta equilibria ($\beta_T > 50\%$) with self-driven current fractions up to 100% have been calculated. Neoclassical tearing modes should be stable. The current drive power and the TF coil Ohmic power remain small enough to project systems with reasonable levels of plant recirculating power. E×B shear stabilization of turbulence will be maximized in the ST and appears strong enough to produce the required levels of confinement. The copper TF coil can be jointed and allows simple full disassembly for replacement of all components, including the centerpost. Estimates of the increase in resistivity of the centerpost from neutron induced transmutation indicate a multi-year lifetime before replacement. The single turn centerpost requires unusual power supplies (few volts, MA currents) which appear possible. The high power density is a challenge to the divertor.

A possible ST fusion development path is shown in Fig. 3. The advanced tokamak physics presently being explored in DIII-D and other higher A devices and results from

START, MAST, and NSTX could lead to a 5 MA, pilot plant sized proof-of-physics performance device constructed with a multi-turn copper TF coil and running deuterium. Favorable results would lead to a pilot plant using DT of the same size but at $I_p = 15$ MA. The step to single-turn TF centerpost technology with no OH-coil would occur here. The pilot plant goal would be $Q_{PLANT} = 1$. The pilot plant could just be scaled up by a factor 2 to 3 to realize a power plant with $Q_{PLANT} \sim 5$ and 1000 to 2000 MW net electric output. Another doubling of the size might bring superconducting TF coil D–He³ (or DT) systems into play.

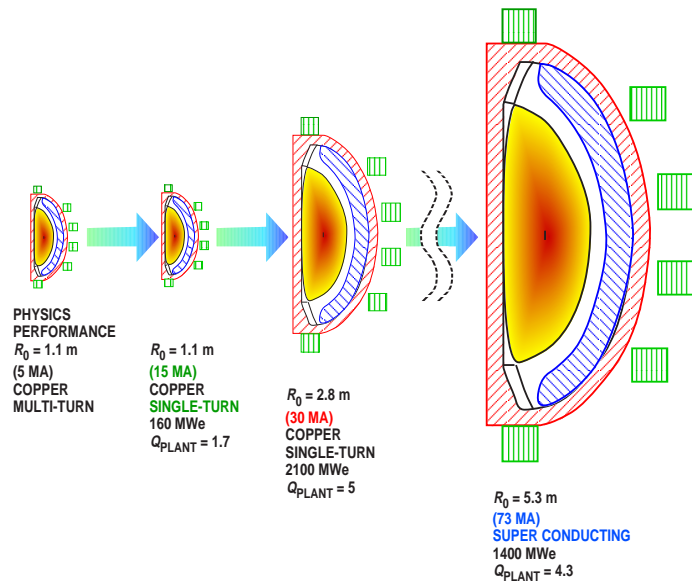


Fig. 3. Possible ST fusion development steps.

ACKNOWLEDGMENT

Work supported by General Atomics and the U.S. Department of Energy under Contract No. DE-AC03-89ER51114.

REFERENCES

- [1] Y-K.M. Peng and D.J. Strickler, Nucl. Fusion **26** (1986) 769.
- [2] Y-K.M. Peng and J.B. Hicks, "Engineering Feasibility of Tight Aspect Ratio Tokamak (Spherical Torus) Reactors," in Proc. 16th Symp. on Fusion Technology, London, 1990.
- [3] Y-K.M. Peng, et al., Fusion Technol. **29** (1995) 210.
- [4] A.C. Darke, et al., "The Mega Amp Spherical Tokamak," in Proc. 16th Symp. on Fusion Energy, Champaign-Urbana, Illinois, 1995.
- [5] J.H. Chrzanowski, et al., "Engineering Overview of the National Spherical Tokamak Experiment," *ibid.*
- [6] FRC Staff "USTX — The University Spherical Tokamak Experiment," DOE/ER/542-41-159 (1996).
- [7] A. Sykes, Plasma Phys. and Contr. Fusion **36** (1994) B93.
- [8] Y-K.M. Peng, et al., in Proc. 15th Int. Conf. on Plasma Physics and Controlled Nuclear Fusion Research, Seville, Spain, 1994, Vol. 2 (IAEA, Vienna, 1995) p. 643.
- [9] T.C. Hender, et al., *ibid.*
- [10] R.D. Stambaugh, et al., "The Spherical Tokamak Path to Fusion Power," General Atomics Report GA-A22226 (1996); submitted to Fusion Technology.
- [11] R.D. Stambaugh, et al., "The Spherical Torus Approach to Magnetic Fusion Development," in Proc. 16th Int. Conf. on Plasma Physics and Controlled Nuclear Fusion Research, Montreal, Canada, 1996 (IAEA F1-CN-64/G1-2, Vienna) to be published.
- [12] R.L. Miller, et al., "Stability for Bootstrap-Current Driven Low Aspect Ratio Tokamaks," General Atomics Report GA-A22321 (1996); submitted to Phys. of Plasmas.
- [13] R.L. Miller and J.W. vanDam, Nucl. Fusion **28** (1987) 2101.
- [14] L.C. Bernard, et al., Comput. Phys. Commun. **24** (1981) 377.
- [15] J.R. Ferron, et al., Phys. Fluids B **5** (1993) 2532.
- [16] R.D. Stambaugh, et al., Plasma Phys. and Contr. Nucl. Fusion Research **1** (1994) 83.
- [17] E.A. Lazarus, et al., "Higher Fusion Power Gain With Pressure Profile Control in Strongly-Shaped DIII-D Tokamak Plasmas," General Atomics Report GA-A22292 (1996); submitted to Phys. Rev. Lett.

- [18] R.J. La Haye, et al., "Practical Beta Limit in ITER-Shaped Discharges in DIII-D and Its Increase by Higher Collisionality," in Proc. 16th Int. Conf. on Plasma Physics and Controlled Nuclear Fusion Research, Montreal, Canada, 1996 (IAEA, Vienna) to be published.
- [19] H.S. Bosch and G.M. Hale, "Improved Formulas for Fusion Cross-Sections and Thermal Reactivities," Nucl. Fusion **32** (1992) 611.
- [20] J.D. Callen, et al., Phys. Today **45** (1992) 34.
- [21] G. Tonon, "Current Drive Efficiency Requirements for an Attractive Steady-State Reactor," in Proc. Workshop on Tokamak Concept Improvement, Varenna, Italy, 1994, p. 233.
- [22] P.N. Yushmanov, et al., Nucl. Fusion **30** (1990) 1999.
- [23] E.J. Doyle, et al., "Physics of Turbulence Control and Transport Barrier Formation in DIII-D," in Proc. 16th Int. Conf. on Plasma Physics and Controlled Nuclear Fusion Research, Montreal, Canada, 1996 (IAEA F1-CN-64/A6-4, Vienna) to be published.
- [24] T.S. Hahm and K.H. Burrell, Phys. Plasmas **2** (1995) 1648.
- [25] E.T. Cheng, et al., "Study of a Spherical Tokamak Based Volumetric Neutron Source," TSIR-45 (1996).